Research Article | Vol. 14, No. 7 / 1 Jul 2023 / Biomedical Optics Express 3689
Biomedical Optics EXPRESS

POF Smart Pants: a fully portable optical fiber-integrated smart textile for remote monitoring of lower limb biomechanics

LETICIA AVELLAR, ANSELMO FRIZERA, AND ARNALDO LEAL-JUNIOR*

Federal University of Espirito Santo, 29075-910 Vitória, Brazil
leal-junior.arnaldo@ieee.org

Abstract: This paper presents the development of an optical fiber-integrated smart textile used as an instrumented pants for biomechanical and activity recognition. The optical fiber sensor is based on the multiplexed intensity variation technique in which a side coupling between a polymer optical fiber (POF) and light sources with controlled modulation is developed. In addition, the sensor system is integrated into pants, where two POFs with 30 sensors each are placed on the left and right legs of the proposed POF Smart Pants. After the device's fabrication and assembly, the 60 optical fiber sensors are characterized as a function of the transverse displacement on the sensor's region. In this case, each sensor presented its sensitivities (108.03 ± 100 mV/mm), which are used on the sensor normalization prior to the data analysis. Then, the tests with volunteer performing different daily activities indicated the suitability of the proposed device on the assessment of biomechanics of human movement in different activities as well as the spatio-temporal parameters of the gait in different velocity conditions. For activity recognition, a neural network is applied and presented 100% accuracy on the activity recognition. Then, to provide an optimization of the number of sensors, the principal components analysis is applied and indicated a threefold reduction of the number of sensors with an accuracy of 99%. Thus, the proposed POF Smart Pants is a feasible alternative for a low-cost and highly reliable sensor system for remote monitoring of different patients, with the possibility of customizing the device for different users.

1. Introduction

Life expectancy has continuously increased since the early days of human history, which resulted in population aging. From 1950 to 2000, the elderly population (over 65 years) rose from 131 million in 1950 to 418 million in 2000, more than a threefold increase in 50 years [1]. The longevity increase is the reflection of the society evolution with advances on public health, medicine, economy and social development [2]. All these advances contribute to the control of diseases, injuries prevention and reduction of premature deaths. Therefore, many health conditions that were deadly in the past nowadays are treatable or curable. According to United Nations (UN) reports, there are four trends in the global population: (i) population growth, (ii) urbanization, (iii) international migration and the (iv) population ageing [2].

The continuous population ageing and the evolution as well as the widespread of the technology in general, but mostly in sensors technologies have enable the development of wearable sensors technologies. Such new advances lead to increasing demands on the sensors technologies, especially in terms of wireless connectivity, portability and autonomy [3]. Moreover, there are also increasing demands for new (and high performance) sensors for parameters monitoring in wearable applications for healthcare [4].

In this way, wearable sensors can be used on healthcare applications [5], where the health condition assessment is not limited to clinical environments [6]. Thus, it is also possible

#492796 https://doi.org/10.1364/BOE.492796
Journal © 2023 Received 13 Apr 2023; revised 17 May 2023; accepted 17 May 2023; published 27 Jun 2023

Biomedical Optics EXPRESS

to monitor different physiological parameters for patients at home, especially for the elderly population and people with locomotor disabilities [7]. These parameters can be divided in kinect (or dynamic) and kinematic parameters for a biomechanics perspective to acquire the angle/displacement and torques/forces in the human movement. In addition, the gait, as a key human movement, involves many parameters such as ground reaction forces (i.e. forces applied in the ground), spatio-temporal parameters (which is related to length and times related to the gait) and plantar pressure mapping (i.e. pressure distribution on the feet during gait) [7]. Important parameters for health assessment also include physiological and health-related signals such as pulse oximetry, breath rate, arterial pressure and heart rate. Disturbances or abnormalities in these parameters may be used as indicators to different diseases [8].

Among important parameters for remote monitoring of patients, the assessment and classification of different activities performed by the user provide important data regarding the user daily routine and biomechanics of the movement [9]. In addition, the remote monitoring of patients present important features related to emotional and psychological positive component in monitoring the patient at home instead of hospitals or clinical facilities due to the possibility of performing their daily activities and the sense of independent growth in the community [10]. To that extent, the sensors integration in flexible devices and multifunctional structures.

Optical Fiber Sensing (OFS) technology is based on the interaction of a measurand with the light guided in the optical fiber, which leads to variations in optical signal related to the parameter of interest. The advantages of OFS over traditional electronic sensors include compactness, lightweight, flexibility, immunity to electromagnetic interference, chemical stability and multiplexing capabilities. Since the early studies of OFS in the 70s, there are a growing number of research groups dedicated to the exploration of this technology [11]. Decades of research led to the development of accurate optical fiber sensing, including several application fields: healthcare, robotics, structural health monitoring, environmental monitoring, medicine and many industrial technologies [12]. It is also important to mention that the mechanical and geometrical features of the optical fibers, especially the ones made of polymers, make it possible to integrate it in different textiles and fabrics. Such integration can be performed through stitching [13], loom fabrics [14] and direct integration between fabric layers [15], where all these methods lead to the full integration between the OFS and the textile without harming the textile's flexibility and movement of the user.

The optical fiber sensing approaches are commonly divided into distributed and non-distributed approaches [16]. Among the distributed sensors, there are the continuous and quasi-distributed approaches, where the continuous ones are related to the use of optical time or frequency domain approaches for continuous monitoring of different parameters along the optical fiber [17]. This approach also includes the use of nonlinear effects in the optical fiber such as Raman [18] and Brillouin [19]. However, such sensors need bulk and costly equipment, which is not portable for wearable applications. Some issues related to their dynamic signal acquisition in conjunction with small spatial resolution can also be considered drawbacks in some of these approaches. To that extent, quasi-distributed approaches using fiber Bragg gratings (FBGs) became a popular optical fiber sensing technique for a variety of applications due to their multiplexing capabilities and passive operation [20]. One of the drawbacks of the FBG sensors are related to the signal acquisition units that are generally non-portable and have higher cost. Although efforts have been reported for the development of lower cost and portable interrogators [21], FBGs still need costly equipment for their inscription in optical fibers [22]. For this reason, the development of portable and low cost techniques for distributed (or quasi-distributed) optical fiber sensors have been proposed [23]. To that extent, the development of quasi-distributed sensors using intensity variation-based sensors were proposed [24]. In this case, the development of sensors systems for remote monitoring and wearable applications were proposed throughout the years using the optical fiber integrated in different flexible structures [13].

Biomedical Optics EXPRESS

Artificial Intelligence (AI) is one area of computer science that focuses on the creation of intelligent machines that normally requires human intelligence [25,26]. It includes adaptations, learning processes, planning and even problem solving. AI algorithms are designed to make artificial machines capture, store and analyze massive amounts of data. This actionable intelligence allows for a more real-time decision-making process based on a situation that is as human as possible [25]. The use of artificial intelligence on optical fiber sensors are thoroughly reported throughout the years for applications in industrial process [27] and movement analysis [28]. In these cases, the machine learning algorithms can extent the sensors performances and provide the data classification [28] as well as the regression of different models [29].

This paper presents the development of optical fiber-integrated smart pants for the activities classification and biomechanical assessment. In order to increase the system's usability, the optical fibers are directly integrated in the pants textile, resulting a in a transparent sensor system. In addition, a portable signal acquisition unit is developed and placed inside the pants pocket. The sensor is based on the multiplexing technique for intensity variation sensors, resulting in a quasi-distributed sensor system with 60 measurement points (30 on each leg). A machine learning algorithm is developed to provide the classification of the activities. The contributions of this work are the novel optical fiber-integrated clothing accessory that can directly assess the biomechanics of the lower limbers in conjunction with the possibility of remote classification of many activities of the daily routine in a wearable device that does not harm the user's movement and without the privacy issues of cameras and image-based systems.

2. Materials and methods

The developed smart pants uses intensity variation polymer optical fiber (POF) sensors made of polymethyl methacrylate (PMMA) optical fibers with 1 mm diameter and 10 $\mu\epsilon$ of cladding thickness. The intensity variation technique is one of the simplest sensing techniques employed in the OFS development. In the intensity variation approach, the optical signal is transmitted from a light source through optical fibers and a transducer converts the optical power in electrical power related to the variation of the medium through the light is transmitted [30]. Thus, the sensitivity is related to the sensor alignment. Figure 1(a) shows the intensity variation technique approach, where a physical variation in the optical fiber provokes a power variation in the output, in addition to the fiber attenuation, which is present even in a straight fiber. The main advantages of intensity-variation sensors are the ease of fabrication, simple detection system, simplicity in signal processing and the low-cost performance.

Sensors based on intensity variation can be made by creating sensitive areas in a polymeric optical fiber. In the approach presented in this work, the sensitive area is made by removing the cladding and part of the fiber core through a lateral section. This increases the sensitivity and linearity of signal attenuation when the optical fiber is bent. The light losses are due to absorption and frustrated total internal reflection when in contact with the surface [11]. When the bending occurs, the incident angle increases and creates a variation on the transmitted signal. When the sensitive zone of the fiber is bending, there are higher losses due to this POF region that has no cladding, increasing the radiation losses. Another source of loss is the surface scattering caused by the coupling between higher and lower guided modes [30]. Figure 1(b) presents the description of a fiber geometry considered in the POF sensor modeling. The sensitive zone is represented by the section length given by c and the section depth of removed material on the fiber core denoted by p. The optical fiber length in Fig. 1(b) is given by L, meanwhile the optical fiber diameter is d, and the curvature radius is R.

The setup of the Fig. 1(a) represents an individual sensor, since the whole fiber comprises an unique measurement point and it is not possible to identify where the physical variation was performed. With the creation of the sensitive zone, the sensor consists of this lateral section, and it also represents a punctual sensor. However, it is possible to achieve a quasi-distributed

Biomedical Optics EXPRESS

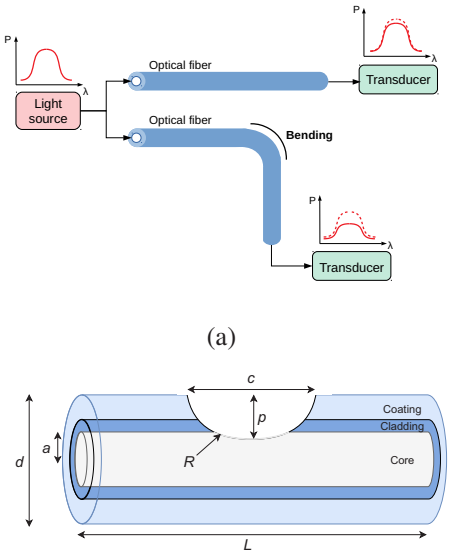

Fig. 1. (a) Intensity variation technique approach: a straight fiber with an attenuation in the output, and a bending in the fiber with a high power variation in the output provoked by the physical variation. (b) Schematic representation of the sensitive zone.

sensor using a multiplexing technique in intensity variation-based sensors [23]. The multiplexing technique consists of laterally coupling light sources, i.e. light emitting diodes (LEDs), to lateral sections, and photodetectors at the fiber ends. An aluminum foil can be placed on the end facet of the fiber to increase the reflectivity, and hence increase the optical power in the phototransistor. Each LED side-coupled to the respective lateral section represents one sensor, which leads to discrete points along the fiber, i.e. a quasi-distributed system. The LEDs activation is time multiplexed, thus each LED is activated at time and its response is acquired by the photodetector, and in the end all the sensors' responses are acquired by a microcontroller. In this way, it is possible to identify the physical variation applied to all these points (sensors) in the fiber. Figure 2 presents the setup of the intensity variation-based quasi-distributed sensors using the multiplexing technique.

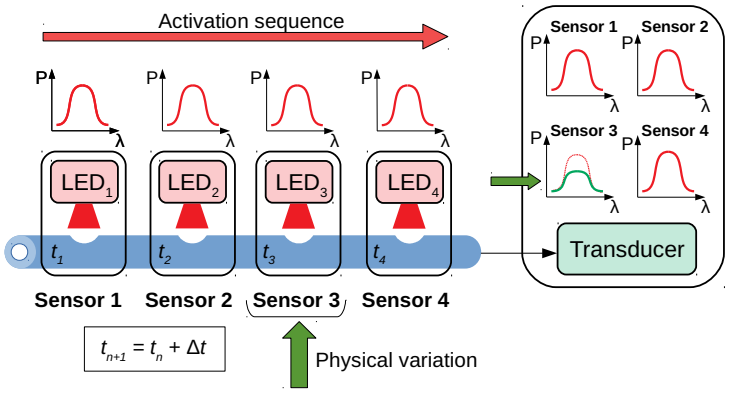

Fig. 2. Multiplexing technique for intensity variation-based sensors.

Biomedical Optics EXPRESS

In this case, two POFs with 30 lateral sections each are positioned on a fabric together with two addressable RGB LED Strips (1 m, 60 LEDs) in which the LED activation and its color are controlled via a communication bus. The flexible LED strip used as the light source are laterally coupled to the lateral sections of the POF in both right and left legs. It is also worth to mention that a Polydimethylsiloxane (PDMS) resin is applied on the LED strip and POF to guarantee the positioning of the lateral sections on the LED regions as well as to avoid misalignment between both components. Then, the textiles with each POF-embedded system are sewed to the back part of neoprene pants. Therefore, each leg of the instrumented pants has 30 sensors positioned on the back region of the pants. The microcontroller FRDM-KL25Z (NXP Semiconductors, Netherlands) controls the LED activation sequence in a way that only one light source is activated at a time. In addition, 16-bit analog-to-digital converters built into the microcontroller are connected to four IF-D92 photodetectors (Industrial Fiber Optics, USA) for optical-to-electrical conversion. Figure 3 presents a photograph and schematic representation of the proposed POF-embedded smart pants.

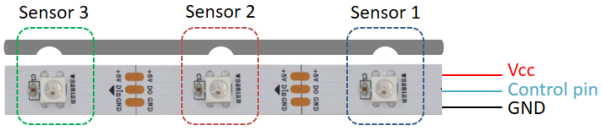

(a)

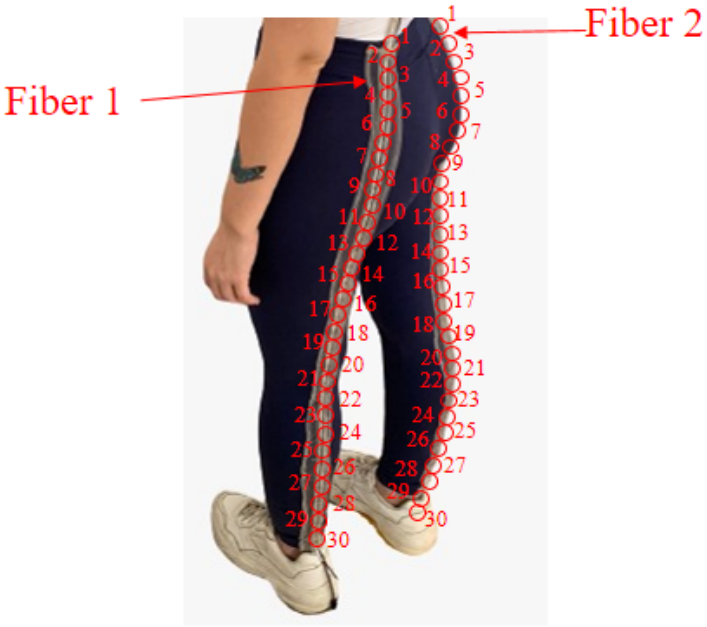

(b)

Fig. 3. (a) POF Smart Pants Sensors system schematic. (b) Identification of the sensors system incorporated in the pants.

The first step on the POF smart pants application is the sensor characterization as a function of the applied displacement. In this case, the sensor regions of the Smart Pants are positioned in a universal testing machine, where controlled transverse displacements are applied on each sensor. Such configuration enables the flexion of each sensor, which is a stress/strain state similar to

Biomedical Optics EXPRESS

the one that can be obtained in the movement analysis. The setup for transverse displacement characterization is presented in Fig. 4, where the vertical displacement in the range of 1 *mm* to 5 *mm* is directly applied on each sensor. The results of this characterization enable the assessment of the sensor sensitivities, which are used on the data normalization prior to the application of the machine learning algorithms.

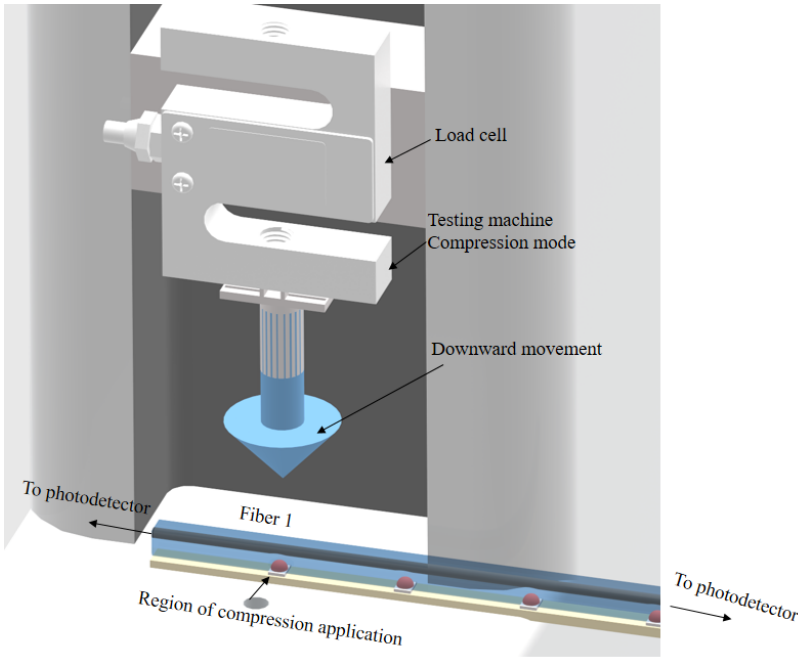

Fig. 4. Curvature characterization setup.

After the sensors characterization, the application on the activities monitoring is proposed. It is important to mention that all volunteers informed consent and the protocols were approved by Research Ethics Committee through the National Commission in Research Ethics – CONEP - (Certificate of Presentation for Ethical Appreciation - CAAE: 41368820.3.0000.5542). Moreover, 7 different activities involving the lower limbs are performed to evaluate the ability of the smart pants in the identification of different movements, as shown in Fig. 5. The activities consists of: (i) walking slow, (ii) walking fast, (iii) squatting, (iv) sitting on a chair, (v) sitting on the floor, (vi) front kick and (vii) back kick. A feed-forward neural network (FFNN) is designed to perform the classification of the 7 activities using the 60 sensors (30 for each leg) as input data. In addition, a principal components analysis (PCA) technique is used to select the most significant sensors and to reduce the number of sensors in the system, which enables the possibility of optimizing the number of sensors and their positioning, resulting in simpler assembly/manufacturing of the system as well as lower computational cost on the signal processing.

The FFNN is a simple type of neural network commonly employed in several applications. The FFNNs have three main layers: input layer, hidden layer, and output layer, as shown in Fig. 6. The input layer is connected to the hidden layers, which are connected to the output layer. The raw data comprise the input layer. There are weights on the connections between the input and hidden layers, and these weights combined with the input layer determine the activities of the hidden units. Similarly, there are weights on the connections between the hidden layers and output layer, and these weights combined with the hidden layers determine the activities of the output layer. The advantage of the FFNN architecture is the ability of the hidden layers in choosing their

Biomedical Optics EXPRESS

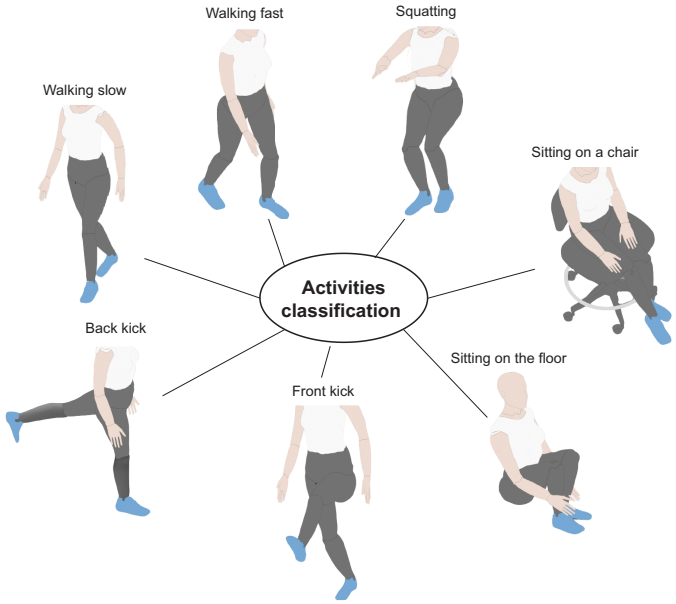

Fig. 5. Activities recognition protocol for the user with the POF Smart Pants.

representations of the inputs by suitably modifying these weights [31]. Considering, Fig. 6, x_1 and x_2 are the inputs from each leg, where each input is a matrix with 30 vectors, one for each sensor of the respective leg.

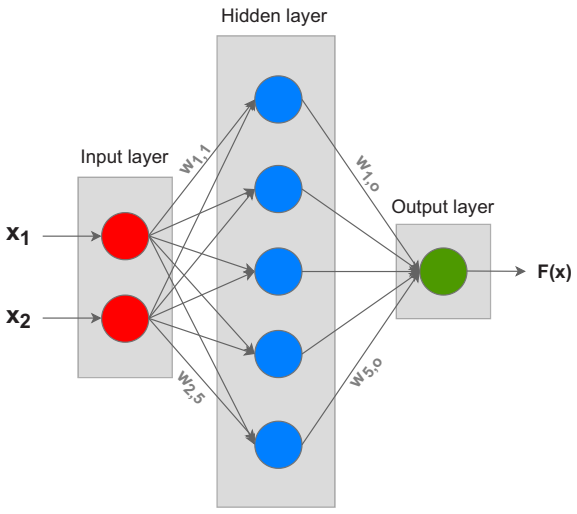

Fig. 6. FFNN architecture used on the activity classification of the POF Smart Pants.

After training, the network learns to recognize certain inputs and returns the correct outputs. Therefore, the objective of the network training algorithm is to build a mapping between the input-outputs samples to form the relationship. This mapping could be a classifier (in classification problems) or a regression function (in approximation problems). For a single training example, the loss error is computed to measure the performance of this sample. The average of the loss

Biomedical Optics EXPRESS

function of the entire training set is called cost function [32]. A cost function is introduced to measure the performance of the neural network. The commonly used cost function is the mean squared error (MSE). Different types of loss function are used in the literature, such as root mean squared error (RMSE) loss or mean absolute error (MAE) loss, for regression loss functions, and binary cross-entropy or categorical cross-entropy, for classification loss functions.

Cross-entropy is category of probability-based loss functions [33]. For binary classification, the binary cross-entropy loss function measures how distant from the true value (which is either 0 or 1) the prediction is for each of the classes and then averages these class errors to obtain the final loss [32]. For multi-class classification, the categorical cross-entropy loss function is applied when the output can be classified as categorical classes. A technique called one-hot encoding is employed in multi-class classification to convert the categorical class to binary format, and the distribution of the predicted and true labels are compared [32]. The standard categorical cross-entropy (CCE) function is defined in Eq. (1), where N is the number of training samples, K is the number of classes, y_n^k is the target label for sample n for class k, x_n is the input for sample n and h_θ is the model with neural network weights θ [32].

$$CCE = -\frac{1}{N}\sum_{k=1}^{K}\sum_{n=1}^{N} y_n^k \cdot log(h_\theta(x_{n,k})) \tag{1}$$

PCA is a technique from the field of linear algebra that converts an attribute set to a new dataset linearly uncorrelated, obtained from the linear combination of the original attributes, so-called principal components. As the principal components have a sample-like pattern with a weight for each attribute, we can use the weights to visualize the influence of each attribute on the dataset [34]. Considering the matrix X_{nxD}, in which the rows represent the samples and the columns represent the attributes, each sample is normalized by subtracting the attribute mean (μ_j) and dividing by the attribute standard deviation (σ_j), as shown in Eq. (2).

$$\hat{x}_{i,j} = \frac{x_{i,j} - \mu_j}{\sigma_j}, \qquad j = 1, 2, \ldots, d \qquad i = 1, \ldots, N \tag{2}$$

With the new matrix X (with mean 0), the correlation matrix C is calculated by using the Eq. (3). From this matrix, the eigenvalues (λ) and eigenvectors (V) are obtained.

$$C = \frac{1}{(N-1)}\hat{X}^T\hat{X} \tag{3}$$

For the dimensionality reduction, the k eigenvectors associated to the largest eigenvalues are selected to compose the new dataset (Ω_x), calculated by the Eq. (4). The k eigenvectors are defined by analyzing the variance explained by each principal component, in which the variance might be higher than 99%, and the number of attributes is reduced. Then, the variance explained can be checked by analyzing the Pareto chart, which presents the accumulative variance explained according to the principal components

$$\Omega_X^T = X \cdot V_{Nxk} \tag{4}$$

In this way, by using the PCA technique it is possible to reduce the computational costs by maintaining similar classification performance, which is interesting for online applications such as the ones proposed in the POF Smart Pants.

3. Results and discussions

Results of the sensors characterization showed different sensors sensitivities. This difference is related to the manufacturing process, which eventually presents minor differences between

Biomedical Optics EXPRESS

sensors, since lateral section parameters (length and depth) as well as the distance between the LED and the optical fiber's lateral section may have small differences for each sensor. All the sensors responses in the characterization are linear fitted (R^2>0.9). Tables 1 and 2 present the sensitivities (mV/mm) of the sensors positioned in the both sides of the pants. It is possible to observe the huge differences between the sensors sensitivities. Fabrication stages such as the sensitive zone creation and the encapsulation of clear urethane rubber mixture can lead to differences between sensors, due to the low precision to achieve the same lateral section parameters and the same coupling of the sensitive zones to their respective LEDs during the encapsulation. However, the differences between sensors can be solved with the sensors normalization as a function of their sensitivities.

Table 1. Sensitivities of sensors in the fiber 1.

Sensor	Sensitivity (mV/mm)	Sensor	Sensitivity (mV/mm)
1	568.09	16	1.43
2	34.07	17	1.88
3	25.67	18	2.25
4	9.22	19	2.28
5	15.64	20	2.15
6	13.70	21	31.68
7	11.80	22	27.19
8	7.32	23	18.33
9	20.36	24	173.24
10	127.30	25	160.93
11	34.39	26	200.21
12	16.01	27	52.11
13	14.99	28	22.50
14	7.31	29	54.63
15	4.22	30	61.98

After the sensor characterization, the volunteers (wearing the the POF Smart Pants) are asked to perform different movements and activities. In this case, the sensors responses are analyzed for the different activities presented in Fig. 5, where the sensors responses are normalized as function of their sensitivities presented in Table 1 for the sensors in the left leg, whereas Table 2 shows the sensitivities of the sensors of the right leg. The sensors at similar positions comparing right and left legs presented different sensitivities, since the sensitivity of each sensors has higher correlation with the thickness of the PDMS layer as well as the lateral section parameters than with the position along the smart pants. Thus, the manufacturing procedures of the sensor system (discussed in Section 2) can lead to differences in the sensors responses due to minor variations in the lateral section parameters in the POF, which result in variations in the sensor response, as depicted in [35]. Furthermore, the thickness of the PDMS layer can lead to differences in the sensitivity, since such layer acts as a diaphragm structure in the sensor system, where the thickness plays a key role in the sensor sensitivity [36]. Therefore, the minor deviations in the PDMS thickness in the manufacturing process can also lead to major deviations in the sensors' sensitivities. The sensors responses are grouped by the similarities of the activities in order to provide the differences in the responses for similar activities, e.g., the squatting, sitting on a chair and sitting on the floor activities are grouped as well as the walking fast and slow and front/back kicks. Thus, three groups of activities are analyzed.

Figure 7(a) presents the time response of sensors 20 for the walking activities. These sensors were chosen due to their positioning considering the user's leg, where sensor 20 is close to the

Biomedical Optics EXPRESS

Table 2. Sensitivities of sensors in the fiber 2.

Sensor	Sensitivity (mV/mm)	Sensor	Sensitivity (mV/mm)
1	19.42	16	4.23
2	334.59	17	13.10
3	52.97	18	152.73
4	15.42	19	366.77
5	68.48	20	509.77
6	21.14	21	400.92
7	305.07	22	513.21
8	200.43	23	370.50
9	29.33	24	9.62
10	224.49	25	42.31
11	283.82	26	26.45
12	239.28	27	7.91
13	388.83	28	19.84
14	106.35	29	2.77
15	24.96	30	4.17

knee region of the volunteer. Thus, the sensors responses resemble the dynamics of such limbs during the gait cycle, as can be compared with conventional curves in the literature [37]. In addition, the Fig. 7(b) shows the fast Fourier transform (FFT) of the periodic curves obtained in all sensors responses. Such responses are related to the cadence in the gait analysis in which the peaks of the frequency spectrum are related to the cadence of the gait (i.e., number of steps per unit of time - seconds or minutes), an important spatio-temporal parameter for gait analysis.

The squatting-related activities (squatting, sitting on the chair and sitting on the floor) are presented in Figs. 8(a), where it is possible to observe the differences in the sensors responses for each case. The sensors of the trunk region presented higher variations in the sitting on the chair and floor applications, since there is the contact of the sensor on the chair (or floor). Such contact does not occur in the case of the squatting activity. Another difference between the activities is related to the higher displacements on the sensors of the knee region (sensor 20) when the sitting on the chair and sitting on the floor activities are considered, due to the necessity of higher flexion angles on the knee region when the volunteer sits on the floor. Furthermore, the kick-related activities responses are presented in Fig. 8(b). In this case, the comparison between the sensors responses for front and back kicks indicated the differences in the displacement of the hip region, which is expected to present opposite directions in the displacement vector related to the movement direction.

Considering the differences in the sensors responses for all performed activities. The results of the FFNN classification are presented in Fig. 9. The accuracy and the loss in 40 epochs are 100% and 0, respectively, which demonstrates that all testing data were correctly classified using the input data from 60 sensors (30 of each leg). In this case, the predefined activities are compared with the sensors responses in the training phase of the algorithm, than, in the testing/validation phases, the activities are estimated from the sensors responses following the trained model. The accuracy on the activity estimation is obtained by comparing the correctly predicted activities (and samples) of each case and the total number of samples. Thus, a 100% accuracy indicates that all activities are correctly estimated/predicted in all cases. This result shows that the number of sensors can be overestimated, since high accuracy can be achieved with lower number of sensors, which leads to an easier system fabrication. Moreover, excessive number of features in the classification introduces additional computational complexity, which can be solved by

Biomedical Optics EXPRESS

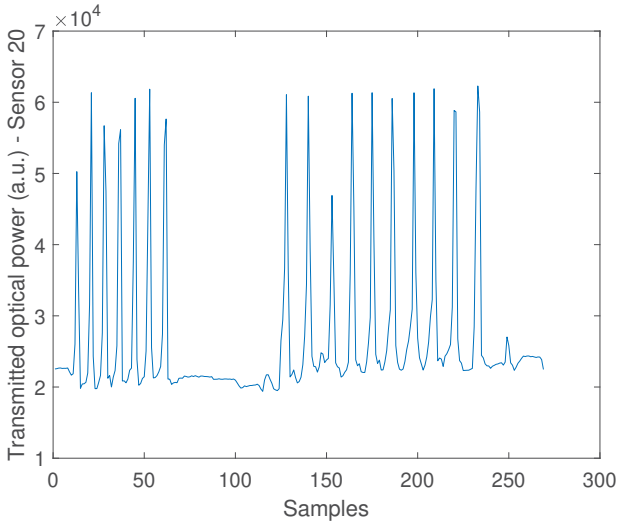

(a)

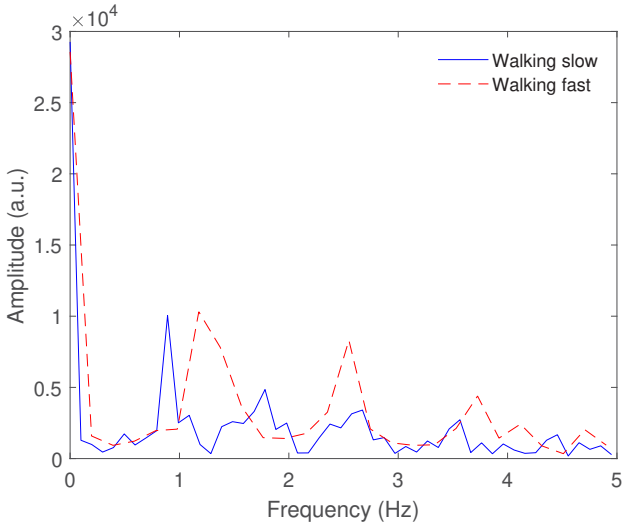

(b)

Fig. 7. POF Smart Pants responses (Sensor 20) for walking activities. (a) Time-domain signal. (b) FFT.

reducing the data dimensionality maintaining the high classification performance. To that extent, the dimensionality reduction using the PCA leads to a reduction in the computational effort, since there is a reduction on the number of input features in the model based on the linear combination of the sensors. From this linear combination, it is possible to obtain the sensors positions (on both right and left legs) that have higher significance on the activities classification, which lead to the possibility of reducing the number of sensors in the POF Smart Pants. However, the reduction in the number of sensors can affect the activities prediction accuracy. For this reason, the number of components in the sensor system is analyzed as a function of the variance, where the optimal number of components is the smaller number of components that result in a variance above 99%.

Biomedical Optics EXPRESS

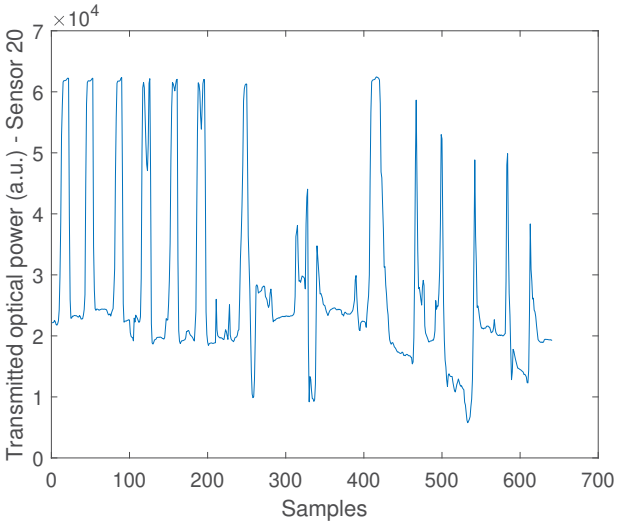

(a)

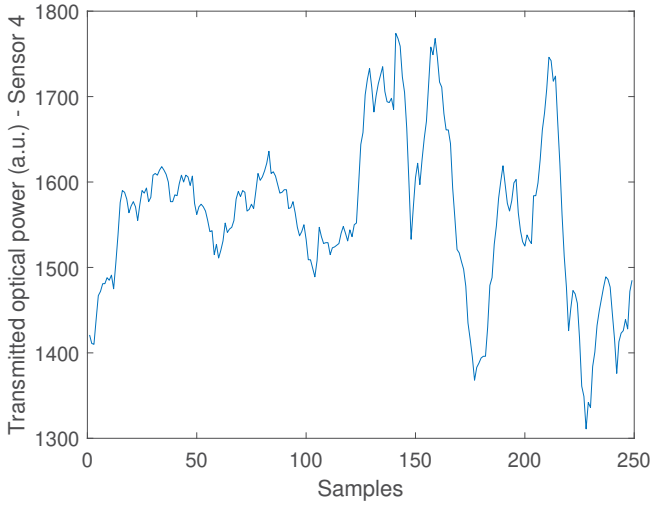

(b)

Fig. 8. POF Smart Pants responses for (a) squatting activity (sensor 20). (b) Kick activity (Sensor 4).

In order to optimize the number of sensors, the PCA technique is employed on the sensors responses. By applying the PCA technique to reduce the dimensionality of the classification input data, the results showed that the reduction to 20 principal components led to variance explained of 99.16%, i.e., a third of the number of new features (principal components) represents more than 99% of the data variance in the classification, as presented in Fig. 10. Thus, if the activities recognition/classification are strictly concerned, there is the possibility of reducing the number of sensors in the system, which result in smaller computational burden and easiness of fabrication.

Due to the high accuracy of 100% and the high variance explained using only 20 principal components, a selection of the most significant weights (resulted from the PCA) is performed. This

Biomedical Optics EXPRESS

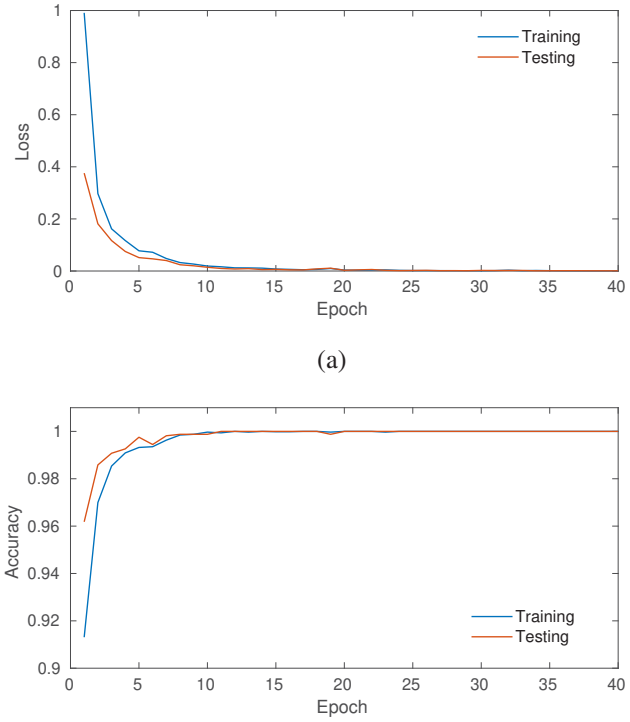

Fig. 9. Metrics of the FFNN model with 40 epochs for activities classification. (a) Loss. (b) Accuracy

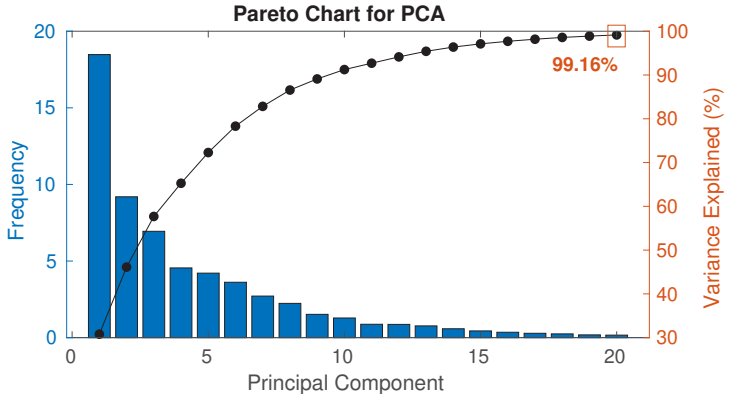

Fig. 10. Pareto chart for the PCA technique.

selection indicates the most significant sensors without significantly decreasing the classification performance. The selected most significant sensors of the fiber 1, as well as the fiber 2, are: 7, 8, 10, 14, 17, 18, 19, 22, 26, 28 and 29. These 11 indices are related to LED's numbering on the addressable LED strip (top to bottom), as showed in the Fig. 11(a), with a total of 22 sensors. This selection illustrates the sensors, which present more variability in their responses during the performed activities.

Biomedical Optics EXPRESS

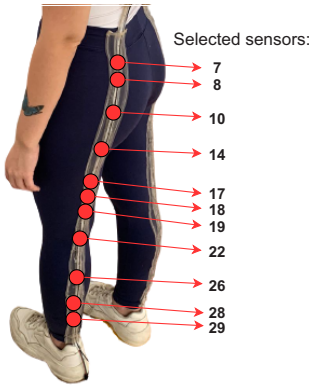

(a)

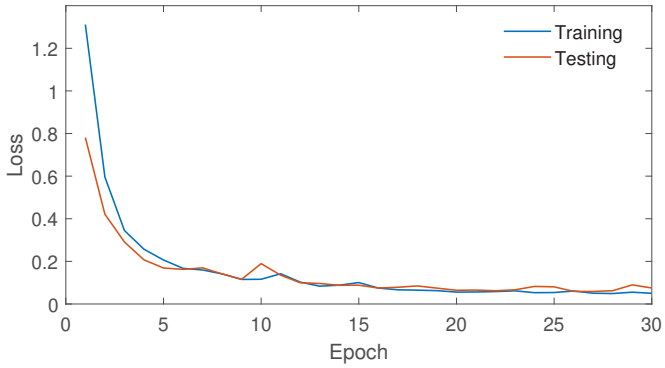

(b)

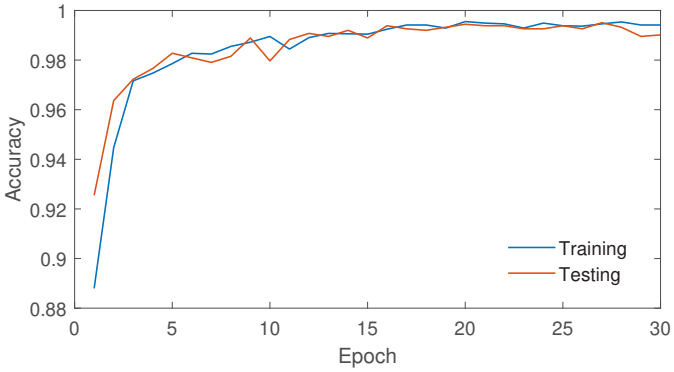

(c)

Fig. 11. (a) Selected sensors by analyzing the principal components weights resulted from the PCA technique. Metrics of the FFNN model with 30 epochs for activities classification after the sensors selection. (b) Loss. (c) Accuracy

After the sensors selection, the FFNN-based classification process is repeated with 30 epochs, since the preliminary classification process using 40 epochs quickly stabilized and it was not necessary to use so many epochs. The accuracy using 22 sensors converged to 99%, approximately,

Biomedical Optics EXPRESS

whereas the loss converged to 0.075, as shown in Figs. 11(b) and (c), respectively. These results showed the possibility of decreasing the number of the sensors, facilitating the manufacturing process and decreasing the data processing cost, providing a similar classification performance. In addition, such result in the number of sensors can lead to lower cost of the sensor system. In this case, considering the cost of the components used in the POF Smart Pants, the cost of entire system is around 80 USD.

4. Conclusion

This paper presented the development and application of a POF-integrated smart pants for the assessment of biomechanical and activity recognition. The optical fiber sensors are based on the multiplexed intensity variation technique in each two POF cables with 30 sensors each are embedded in the left and right legs of the pants. Each sensor is characterized as a function of the transverse displacement in order to obtain the sensors sensitivities, which are used on the data normalization. Then, a volunteer is asked to perform different daily activities wearing the POF Smart Pants. The results show the ability of the proposed device to acquire the data at different movement conditions and the possibility of estimating the gait spatio-temporal parameters. In addition, a FFNN algorithm is applied for the data analysis, where the activities performed by the user can be classified. The classification results show a 100% accuracy on the data classification using all 60 sensors, which not only demonstrate the feasibility of the proposed device, but also open the possibility of further optimization of the number of sensors for the activity classification. To that extent, the PCA was applied and resulted in a threefold reduction of the number of sensors needed to obtain 99% accuracy in the activities classification. Therefore, the proposed approach is a low-cost, highly integrated and fully portable method for lower limb biomechanics analysis and activities classification that can be applied on remote monitoring of different patients with the additional possibility of customizing the number of sensors according with the applications and users. Future works include the integration of the proposed device in a smart environment and the use of additional sensors systems for movement reconstruction.

Funding. Financiadora de Estudos e Projetos (2784/20); Conselho Nacional de Desenvolvimento Científico e Tecnológico (304049/2019-0, 310709/2021-0, 403753/2021-0, 440064/2022-8); Fundação de Amparo à Pesquisa e Inovação do Espírito Santo (1004/2022 P: 2022-6PC5F, 2021-TBG0J, 2022-2JV95, 2022-C5K3H, 2022-D48XB).

Disclosures. The authors declare no conflicts of interest.

Data availability. Data underlying the results presented in this paper are not publicly available at this time but may be obtained from the authors upon reasonable request.

References

1. P. Uhlenberg, "Handbook of Population Ageing," vol. 1 (2009).
2. P. D. United Nations, Department of Economic and Social Affairs, "World Population Ageing 2019 (2019)," highlights ed.
3. G. H. Lee, H. Moon, H. Kim, G. H. Lee, W. Kwon, S. Yoo, D. Myung, S. H. Yun, Z. Bao, and S. K. Hahn, "Multifunctional materials for implantable and wearable photonic healthcare devices," Nat. Rev. Mater. **5**(2), 149–165 (2020).
4. C. Gonçalves, A. F. da Silva, J. Gomes, and R. Simoes, "Wearable e-textile technologies: A review on sensors, actuators and control elements," Inventions **3**(1), 14 (2018).
5. A. Nag, S. C. Mukhopadhyay, and J. Kosel, "Wearable Flexible Sensors: A Review," IEEE Sens. J. **17**(13), 3949–3960 (2017).
6. I. Korhonen, J. Pärkkä, and M. V. Gils, "Health Monitoring in the Home of the Future," IEEE Engineering in Medicine and Biology Magazine **22**(3), 66–73 (2003).
7. S. Majumder, T. Mondal, and M. J. Deen, "Wearable sensors for remote health monitoring," Sensors (Switzerland) **17**(12), 130 (2017).
8. M. Böhm, J. C. Reil, P. Deedwania, J. B. Kim, and J. S. Borer, "Resting heart rate: Risk indicator and emerging risk factor in cardiovascular disease," Am. J. Med. **128**(3), 219–228 (2015).
9. A. Ahad, M. Tahir, and K. L. A. Yau, "5G-based smart healthcare network: Architecture, taxonomy, challenges and future research directions," IEEE Access **7**, 100747–100762 (2019).

Biomedical Optics EXPRESS

10. L. Na and J. E. Streim, "Psychosocial Well-Being Associated With Activity of Daily Living Stages Among Community-Dwelling Older Adults," Gerontology and Geriatric Medicine **3**, 233372141770001 (2017).
11. L. Bilro, N. Alberto, J. L. Pinto, and R. Nogueira, "Optical Sensors Based on Plastic Fibers," Sensors **12**(9), 12184–12207 (2012).
12. G. Rajan, "Optical fiber sensors: Advanced Techniques & Applications," 1 (2015).
13. A. Leal-Junior, L. Avellar, A. Frizera, and C. Marques, "Smart textiles for multimodal wearable sensing using highly stretchable multiplexed optical fiber system," Sci. Rep. **10**(1), 13867 (2020).
14. M. Rothmaier, B. Selm, S. Spichtig, D. Haensse, and M. Wolf, "Photonic textiles for pulse oximetry," Opt. Express **16**(17), 12973 (2008).
15. L. Avellar, G. Delgado, C. Marques, A. Frizera, A. Leal-Junior, and E. Rocon, "Polymer Optical Fiber-Based Smart Garment for Impact Identification and Balance Assessment," IEEE Sens. J. **21**(18), 20078–20085 (2021).
16. Y. Mizuno, A. Theodosiou, K. Kalli, S. Liehr, H. Lee, and K. Nakamura, "Distributed polymer optical fiber sensors: a review and outlook," Photonics Res. **9**(9), 1719 (2021).
17. Z. Ding, C. Wang, K. Liu, J. Jiang, D. Yang, G. Pan, Z. Pu, and T. Liu, "Distributed Optical Fiber Sensors Based on Optical Frequency Domain Reflectometry: A review," Sensors **18**(4), 1072 (2018).
18. L. Schenato, "A Review of Distributed Fibre Optic Sensors for Geo-Hydrological Applications," Appl. Sci. **7**(9), 896 (2017).
19. Y. Mizuno, N. Hayashi, H. Fukuda, K. Y. Song, and K. Nakamura, "Ultrahigh-speed distributed Brillouin reflectometry," Light: Science & Applications **5**(12), e16184 (2016).
20. C. Broadway, R. Min, A. Leal-Junior, C. Marques, and C. Caucheteur, "Toward Commercial Polymer Fiber Bragg Grating Sensors: Review and Applications," J. Lightwave Technol. **37**(11), 2605–2615 (2019).
21. C. A. R. Diaz, A. G. Leal-Junior, L. M. Avellar, P. F. C. Antunes, M. J. Pontes, C. A. Marques, A. Frizera, and M. R. N. Ribeiro, "Perrogator: A Portable Energy-Efficient Interrogator for Dynamic Monitoring of Wavelength-Based Sensors in Wearable Applications," Sensors **19**(13), 2962 (2019).
22. C. A. F. Marques, R. Min, A. Leal Junior, P. Antunes, A. Fasano, G. Woyessa, K. Nielsen, H. K. Rasmussen, B. Ortega, and O. Bang, "Fast and stable gratings inscription in POFs made of different materials with pulsed 248 nm KrF laser," Opt. Express **26**(2), 2013 (2018).
23. A. G. Leal-Junior, C. R. Díaz, C. Marques, M. J. Pontes, and A. Frizera, "Multiplexing technique for quasi-distributed sensors arrays in polymer optical fiber intensity variation-based sensors," Optics & Laser Technology **111**, 81–88 (2019).
24. L. Avellar, A. Leal-Junior, C. Diaz, C. Marques, and A. Frizera, "POF smart carpet: A multiplexed polymer optical fiber-embedded smart carpet for gait analysis," Sensors (Switzerland) **19**(15), 3356 (2019).
25. J. Chanchaichujit, A. Tan, F. Meng, and S. Eaimkhong, "Optimization, Simulation and Predictive Analytics in Healthcare," (2019).
26. J. D. Rudie, A. M. Rauschecker, R. N. Bryan, C. Davatzikos, and S. Mohan, "Emerging Applications of Artificial Intelligence in Neuro-Oncology," Radiology **290**(3), 607–618 (2019).
27. K. P. Nascimento, A. Frizera-Neto, C. Marques, and A. G. Leal-Junior, "Machine learning techniques for liquid level estimation using FBG temperature sensor array," Opt. Fiber Technol. **65**, 102612 (2021).
28. L. Avellar, C. Stefano Filho, G. Delgado, A. Frizera, E. Rocon, and A. Leal-Junior, "AI-enabled photonic smart garment for movement analysis," Sci. Rep. **12**(1), 4067 (2022).
29. L. Avellar, M. Silveira, C. A. Diaz, C. Marques, A. Frizera, W. Blanc, and A. Leal-Junior, "Transmission-Reflection Performance Analysis Using Oxide Nanoparticle-Doped High Scattering Fibers," IEEE Photonics Technol. Lett. **34**(16), 874–877 (2022).
30. L. Renqiang, F. Zhuang, Z. Yanzheng, C. Qixin, and W. Shuguo, "Operation Principle of a Bend Enhanced Curvature Optical Fiber Sensor," in *2006 IEEE/RSJ International Conference on Intelligent Robots and Systems*, (IEEE, 2006), pp. 1966–1971.
31. Y. LeCun, Y. Bengio, and G. Hinton, "Deep learning," Nature **521**(7553), 436–444 (2015).
32. Y. Ho and S. Wookey, "The Real-World-Weight Cross-Entropy Loss Function: Modeling the Costs of Mislabeling," IEEE Access **8**, 4806–4813 (2020).
33. L. Li, M. Doroslovacki, and M. H. Loew, "Approximating the Gradient of Cross-Entropy Loss Function," IEEE Access **8**, 111626–111635 (2020).
34. M. Ringnér, "What is principal component analysis?" Nat. Biotechnol. **26**(3), 303–304 (2008).
35. A. G. Leal-Junior, A. Frizera, and M. José Pontes, "Sensitive zone parameters and curvature radius evaluation for polymer optical fiber curvature sensors," Optics & Laser Technology **100**, 272–281 (2018).
36. A. G. Leal-Junior and C. Marques, "Diaphragm-Embedded Optical Fiber Sensors: A Review and Tutorial," IEEE Sens. J. **21**(11), 12719–12733 (2021).
37. C. Kirtley, *Clinical Gait Analysis: Theory and Practice* (Elsevier B.V., London, UK, 2006), 1st ed.